Commun Nonlinear Sci Numer Simulat 15 (2010) 2735–2743

Contents lists available at ScienceDirect

Commun Nonlinear Sci Numer Simulat

journal homepage: www.elsevier.com/locate/cnsns

Short communication

Dynamics of microbubble oscillators with delay coupling

C.R. Heckman [a], S.M. Sah [b], R.H. Rand [c,d,*]

[a] Field of Theoretical and Applied Mechanics, Cornell University, Ithaca, NY 14850, USA
[b] Laboratory of Mechanics, University Hassan II-Aïn Chock, PB 5366 Maârif, Casablanca, Morocco
[c] Department of Mechanical and Aerospace Engineering, Cornell University, Ithaca, NY 14850, USA
[d] Department of Mathematics, Cornell University, Ithaca, NY 14850, USA

ARTICLE INFO

Article history:
Received 12 October 2009
Accepted 15 October 2009
Available online 24 October 2009

Keywords:
Microbubble
Differential delay equation
Perturbation theory
Hopf bifurcation

ABSTRACT

We investigate the stability of the in-phase mode in a system of two delay-coupled bubble oscillators. The bubble oscillator model is based on a 1956 paper by Keller and Kolodner. Delay coupling is due to the time it takes for a signal to travel from one bubble to another through the liquid medium that surrounds them. Using techniques from the theory of differential-delay equations as well as perturbation theory, we show that the equilibrium of the in-phase mode can be made unstable if the delay is long enough and if the coupling strength is large enough, resulting in a Hopf bifurcation. We then employ Lindstedt's method to compute the amplitude of the limit cycle as a function of the time delay. This work is motivated by medical applications involving noninvasive localized drug delivery via microbubbles.

1. Introduction

Delay in dynamical systems is exhibited whenever the system's behavior is dependent at least in part on its history. Many technological and biological systems are known to exhibit such behavior; coupled laser systems, high-speed milling, population dynamics and gene expression are some examples of delayed systems. This paper treats a new application of delay-differential equations, that of a microbubble cloud under acoustic forcing. This work is motivated by medical applications, where microbubbles are used in the noninvasive, localized delivery of drugs. In this process, microbubbles can either be filled with or their surfaces coated with drugs which work best locally. The microbubbles are propagated to the target site and collapsed by a strong ultrasound wave [1,3,9]. Full understanding of the behavior of systems of coupled microbubbles involves taking into account the speed of sound in the liquid, which will lead to a delay in induced pressure waves between the bubbles in a cloud.

The first analysis in bubble dynamics was made by Rayleigh [18]. While in his work he considered an incompressible fluid with a constant background pressure, differential equation models of bubble dynamics in a compressible fluid with time-dependent background pressure were studied by, e.g., Plesset [12], Gilmore [4], Plesset and Prosperetti [13], and by Joseph Keller and his associates [6,7], as well as many contemporaries including, for instance, Lauterborn [8] and Szeri [19,20]. The main object of these studies has been the so-called Rayleigh-Plesset Equation, which governs the radius of a spherical bubble in a compressible fluid:

* Corresponding author. Address: Department of Mechanical and Aerospace Engineering, Cornell University, Ithaca, NY 14850, USA. Fax: +1 607 255 2011.
E-mail address: rhr2@cornell.edu (R.H. Rand).

1007-5704/$ - see front matter
doi:10.1016/j.cnsns.2009.10.017

$$(\dot{a}-c)\left(a\ddot{a}+\frac{3}{2}\dot{a}^2-\Delta\right)-\dot{a}^3+a^{-1}(a^2\Delta)^{\cdot}=0 \tag{1}$$

Here, $\Delta=\rho^{-1}(p(a)-p_0)$, where ρ is the density of the liquid, and p_0 is the far-field liquid pressure. The pressure $p(a)$ inside the bubble is calculated using the adiabatic relation $p(a)=k\left(\frac{4\pi}{3}a^3\right)^{-\gamma}$, where k is determined by the quantity and type of gas in the bubble and γ is the adiabatic exponent of the gas. Next, we nondimensionalize Eq. (1) by setting

$$a=\tilde{a}k_a,\quad t=\tilde{t}k_t,\quad \text{and}\quad c=\tilde{c}(\rho/p_0)^{-1/2} \tag{2}$$

where

$$k_a=(3/(4\pi))^{1/3}(k/p_0)^{1/(3\gamma)},\quad k_t=k_a(\rho/p_0)^{1/2} \tag{3}$$

and obtain the dimensionless equation [6]:

$$(\dot{a}-c)\left(a\ddot{a}+\frac{3}{2}\dot{a}^2-a^{-3\gamma}+1\right)-\dot{a}^3-(3\gamma-2)a^{-3\gamma}\dot{a}-2\dot{a}=0 \tag{4}$$

where we have dropped the tildes on t, a and c for convenience.

Eq. (4) has an equilibrium solution at

$$a=a_e=1 \tag{5}$$

To determine its stability, we set $a=a_e+x=1+x$ and linearize about $x=0$, giving:

$$c\ddot{x}+3\gamma\dot{x}+3c\gamma x=0 \tag{6}$$

Since c and γ are positive-valued parameters, Eq. (6) corresponds to a damped linear oscillator, which tells us that the equilibrium (5) is stable.

Eq. (4) applies only to a single bubble submerged in a fluid field. If there are multiple bubbles submerged, then the bubbles become coupled by the pressure waves induced in the liquid. Therefore, Eq. (4) no longer has the right-hand side equal to zero, but in fact will be driven by some coupling function. This system is illustrated in Fig. 1.

With the introduction of a second bubble, the system under study becomes more complex, with the compressibility of the fluid giving rise to a time delay in the coupling function between the two bubbles:

$$\begin{aligned}(\dot{a}-c)\left(a\ddot{a}+\frac{3}{2}\dot{a}^2-a^{-3\gamma}+1\right)-\dot{a}^3-(3\gamma-2)a^{-3\gamma}\dot{a}-2\dot{a}&=Pf(b(t-T))\\(\dot{b}-c)\left(b\ddot{b}+\frac{3}{2}\dot{b}^2-b^{-3\gamma}+1\right)-\dot{b}^3-(3\gamma-2)b^{-3\gamma}\dot{b}-2\dot{b}&=Pf(a(t-T))\end{aligned} \tag{7}$$

The preponderance of previous work has neglected the time-delay T, thereby reducing Eq. (7) to a standard nonlinear system of differential equations without delay. In these studies, very sophisticated patterns of bubble behavior have been discovered. For instance, assume that bubbles a and b have equilibrium bubble radii a_0 and b_0, respectively, and resonant frequen-

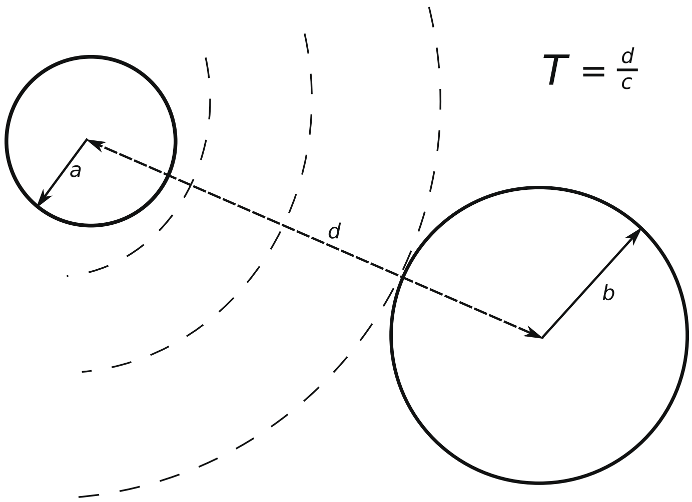

Fig. 1. Two bubbles submerged in a liquid. Note that bubble b also influences bubble a with an induced acoustic wave. Delay $T=d/c$ where d is the distance between bubbles and c is sound speed.

cies ω_a and ω_b respectively. Without loss of generality, assume $a_0 < b_0$; a study of the resonant frequencies of Eq. (4) yields that $\omega_b < \omega_a$. In this case, if an acoustic driver forces both of the bubbles with frequency ω_{ext}, Harkin et al. [5], then

$$\omega_{ext} < \omega_b \Rightarrow \text{bubbles oscillate out of phase} \tag{8}$$

$$\omega_b < \omega_{ext} < \omega_a \Rightarrow \text{bubbles oscillate in phase} \tag{9}$$

$$\omega_a < \omega_{ext} \Rightarrow \text{bubbles oscillate out of phase} \tag{10}$$

Other works have studied the equation that governs translational dynamics of bubbles in a fluid [19,20]. These have built upon previous work, asserting that bubbles oscillating in phase tend to be attracted to one another. Experimental work as accomplished by Yamakoshi et al. [22] has corroborated this finding. These works have not, however investigated the effect of delay on the coupled bubble system.

2. Two coupled bubble oscillators

In this work we consider the dynamics of a system of two coupled bubble oscillators, each of the form of Eq. (4), with delay coupling. Manasseh et al. [10] have studied coupled bubble oscillators without delay. The source of the delay comes from the time it takes for the signal to travel from one bubble to the other through the liquid medium which surrounds them. Adding the coupling terms used in [10], the governing equations of the bubble system are:

$$(\dot{a}-c)\left(a\ddot{a}+\frac{3}{2}\dot{a}^2-a^{-3\gamma}+1\right)-\dot{a}^3-(3\gamma-2)a^{-3\gamma}\dot{a}-2\dot{a}=P\dot{b}(t-T) \tag{11}$$

$$(\dot{b}-c)\left(b\ddot{b}+\frac{3}{2}\dot{b}^2-b^{-3\gamma}+1\right)-\dot{b}^3-(3\gamma-2)b^{-3\gamma}\dot{b}-2\dot{b}=P\dot{a}(t-T) \tag{12}$$

where T is the delay and P is a coupling coefficient. Here we have omitted coupling terms of the form $P_1b(t-T)$ and $P_1a(t-T)$ from Eq. (7), where P_1 is a coupling coefficient [10].

The system (11) and (12) possesses an invariant manifold called the *in-phase manifold* given by $a=b, \dot{a}=\dot{b}$. A periodic motion in the in-phase manifold is called an *in-phase mode*.The dynamics of the in-phase mode are governed by the equation [17]:

$$(\dot{a}-c)\left(a\ddot{a}+\frac{3}{2}\dot{a}^2-a^{-3\gamma}+1\right)-\dot{a}^3-(3\gamma-2)a^{-3\gamma}\dot{a}-2\dot{a}=P\dot{a}(t-T) \tag{13}$$

This equation has the equilibrium $a=a_e=1$. To determine the stability of this equilibrium, we set $a=a_e+x=1+x$ and linearize about $x=0$, giving:

$$c\ddot{x}+3\gamma\dot{x}+3c\gamma x=-P\dot{x}(t-T) \tag{14}$$

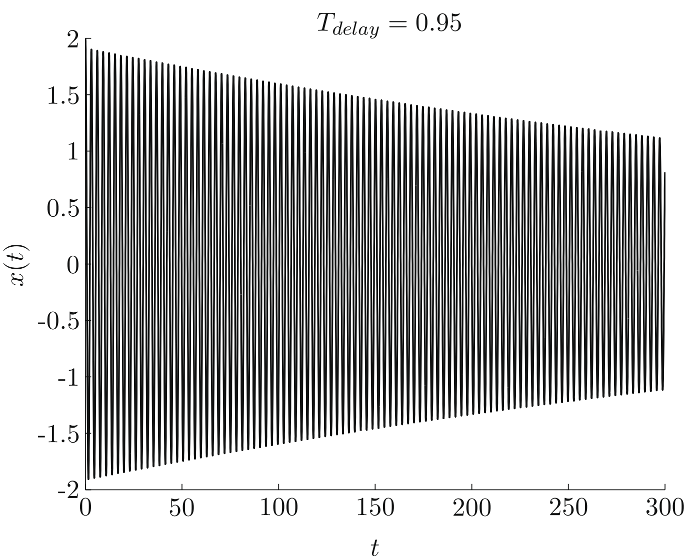

Fig. 2. Numerical integration of the linearized Eq. (14) for the parameters of Eq. (15) with delay $T = 0.95$. Note that the equilibrium is stable.

Before proceeding with an analytical treatment of Eq. (14), we use the MATLAB function `dde23` to numerically integrate (14). We choose the following dimensionless parameters based on the papers by Keller et al.:

$$c = 94, \quad \gamma = \frac{4}{3}, \quad P = 10 \tag{15}$$

Results of the numerical integration for linearized Eq. (14) are shown in Figs. 2 and 3.

Inspection of Figs. 2 and 3 reveals that the equilibrium $a = 1$ loses its stability as the delay T is increased through a critical value T_{cr}. Associated with this periodic motion is its frequency ω_{cr}. From Figs. 2 and 3 we obtain the following approximate values for T_{cr} and ω_{cr}:

$$T_{cr} \approx 1, \quad \omega_{cr} \approx 2 \tag{16}$$

Eq. (14) is a linear differential-delay equation. To solve it, we set $x = \exp \lambda t$ (see [14]), giving

$$c\lambda^2 + 3\gamma\lambda + 3c\gamma = -P\lambda \exp -\lambda T \tag{17}$$

We seek the smallest value of delay $T = T_{cr}$ which causes instability. This will correspond to imaginary values of λ. Thus we substitute $\lambda = i\omega$ in Eq. (17) giving two real equations for the real-valued parameters ω and T:

$$P\omega \sin \omega T = c(\omega^2 - 3\gamma) \tag{18}$$

$$P\omega \cos \omega T = -3\gamma\omega \tag{19}$$

Eq. (19) gives

$$\omega T = \arccos \left(\frac{-3\gamma}{P} \right) \tag{20}$$

whereupon Eq. (18) becomes

$$\omega^2 - \frac{\sqrt{P^2 - 9\gamma^2}\,\omega}{c} - 3\gamma = 0 \tag{21}$$

from which we obtain

$$\omega_{cr} = \frac{\sqrt{P^2 - 9\gamma^2 + 12c^2\gamma} + \sqrt{P^2 - 9\gamma^2}}{2c} \tag{22}$$

which, when combined with (20), gives

$$T_{cr} = \frac{2c \arccos\left(-\frac{3\gamma}{P}\right)}{\sqrt{P^2 - 9\gamma^2 + 12c^2\gamma} + \sqrt{P^2 - 9\gamma^2}} \tag{23}$$

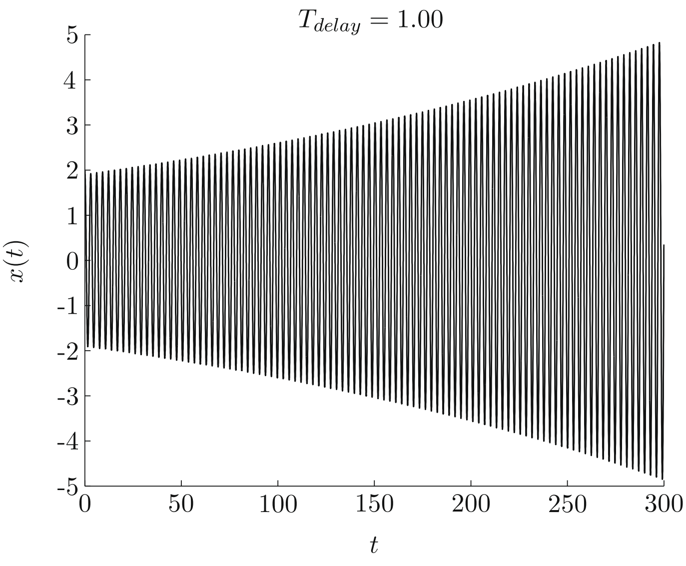

Fig. 3. Numerical integration of the linearized Eq. (14) for the parameters of Eq. (15) with delay $T = 1.00$. Note that the equilibrium is unstable.

For the parameters of Eqs. (15), (22) and (23) give

$$T_{cr} = 0.9673, \quad \omega_{cr} = 2.0493 \tag{24}$$

which agree with the simulations in Figs. 2 and 3, cf. Eq. (16).

Eq. (23) shows that a necessary condition for instability is that the coupling parameter P must satisfy the inequality:

$$P > 3\gamma \tag{25}$$

Eq. (23) gives that as $P \to 3\gamma$, $T_{cr} \to \frac{\pi}{\sqrt{3\gamma}} = 1.622$ for $\gamma = \frac{4}{3}$. Fig. 4 shows a plot of T_{cr} as a function of P for parameters $c = 94$ and $\gamma = \frac{4}{3}$, from Eq. (23). Therefore, for instability of the origin we need both $P > 3\gamma$ and $T > T_{cr}$.

This type of linear DDE analysis of a system of two bubbles has been presented in previous works by other investigators [11,2]. Note that these results are unrealistic in the sense that unbounded behavior is predicted in the unstable case. The

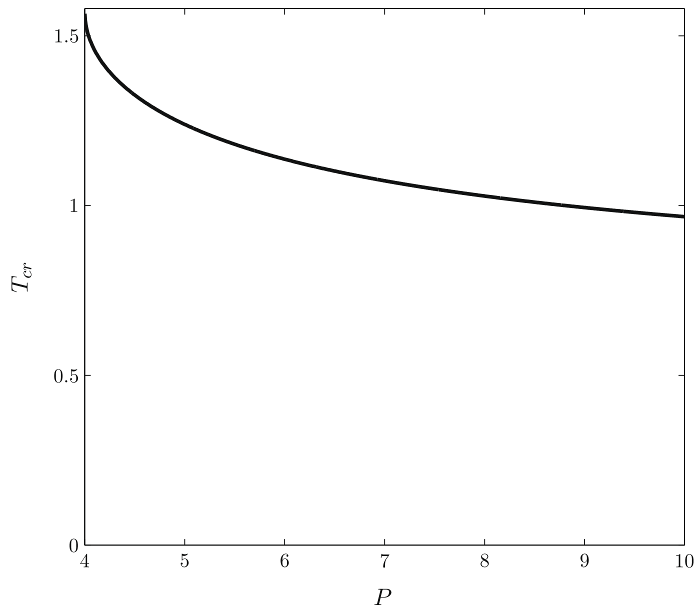

Fig. 4. T_{cr} versus P for parameters $c = 94$ and $\mu = \frac{4}{3}$, from Eq. (23). For $T > T_{cr}$ and $P > 3\gamma$ the origin is unstable and a bounded periodic motion (a limit cycle) exists, having been born in a Hopf bifurcation.

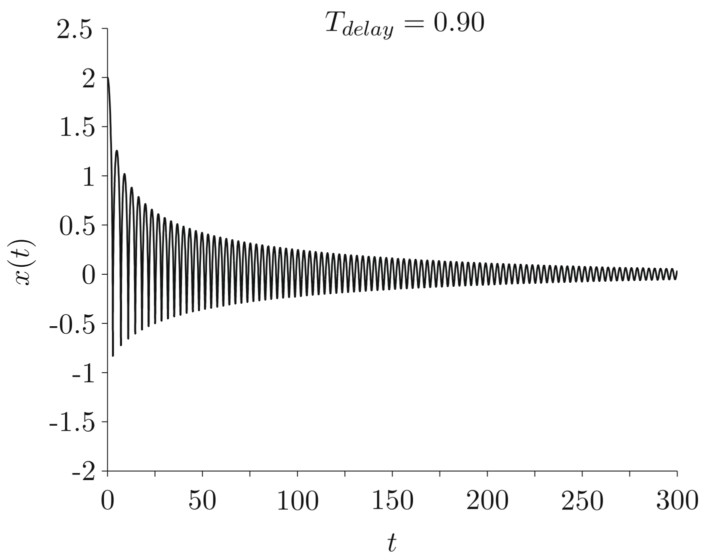

Fig. 5. Numerical integration of Eq. (13) for the parameters of Eq. (15) with delay $T = 0.90$. Note that the equilibrium is stable.

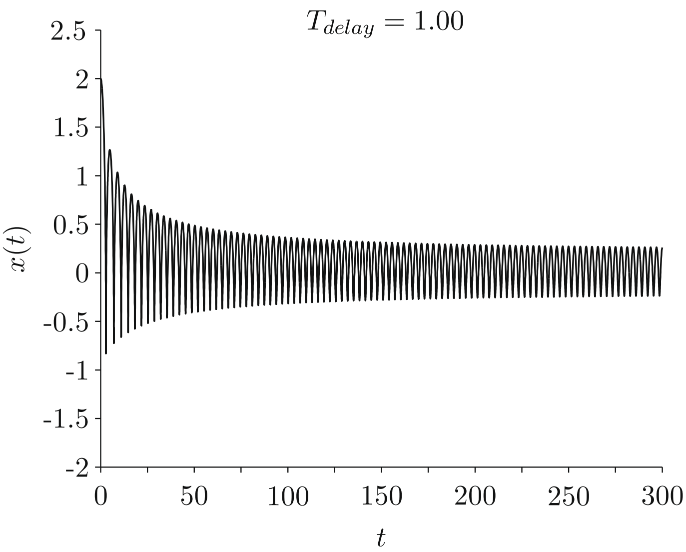

Fig. 6. Numerical integration of Eq. (13) for the parameters of Eq. (15) with delay $T = 1.00$. Note that the equilibrium has become unstable, but that a bounded periodic motion exists indicating a Hopf bifurcation.

original nonlinear Eq. (13) however predicts a bounded periodic motion for $T > T_{cr}$. See Figs. 5 and 6 where Eq. (13) has been numerically integrated. The periodic motion has been born in a Hopf bifurcation [14].

In [17], Rand and Heckman have applied second order averaging [15,16] to the nonlinear bubble Eq. (13). The analysis assumed small delay. The same assumption of small delay was made by Wirkus and Rand [21], where first order averaging was used to study the dynamics of two van der Pol oscillators with delay coupling. In the present work we go beyond [17], and use large delay, perturbing off of T_{cr}. As we show next, we are able to analytically predict the amplitude of the limit cycle in Fig. 7, for example.

3. Perturbations

As the time delay T is increased through T_{cr}, a pair of roots of the characteristic Eq. (17) for the linearized system (14) will cross the imaginary axis with zero real part. As the fixed point at the origin loses hyperbolicity, it will undergo a Hopf bifur-

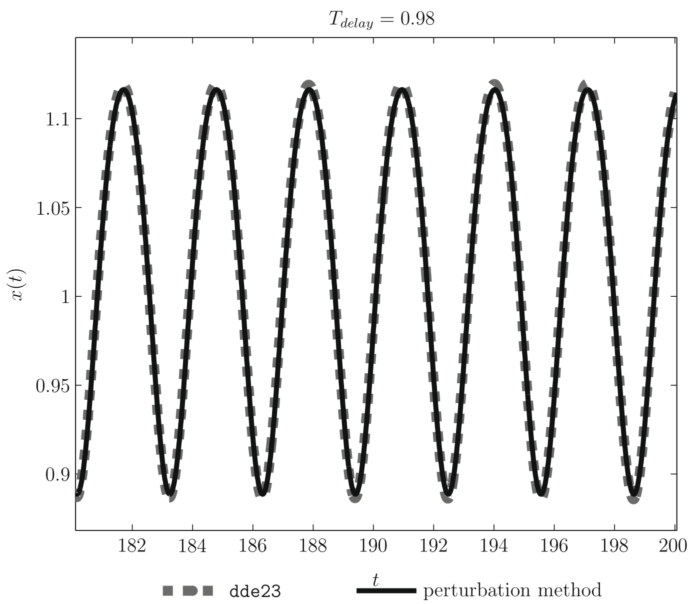

Fig. 7. Perturbation results (solid line) compared against numerical integration (dashed line) of Eq. (13) for the parameters of Eq. (15) with delay $T = 0.98$. The numerical integration results were run for a long time to ensure the limit cycle's amplitude had reached steady state.

cation — and as a result, a limit cycle will be born. This limit cycle will start with zero amplitude and will grow as T is further increased. The relationship between the amplitude of the limit cycle and the value of T may be obtained through use of singular perturbation theory.

The method used here is known as Lindstedt's Method [14], a technique employed to approximate solutions in weakly nonlinear systems by eliminating secular terms. To begin, we perturb Eq. (13) slightly from its equilibrium position by introducing a variable x, which tracks the deviation from equilibrium (recall Eq. (5)):

$$a(t) = 1 + \epsilon x(t) \tag{26}$$

Inserting Eq. (26) into the in-phase mode Eq. (13) yields

$$(\epsilon\dot{x} - c)\left(\epsilon\ddot{x}(\epsilon x + 1) + \frac{3}{2}(\epsilon\dot{x})^2 - (\epsilon x + 1)^{-4} + 1\right) - (\epsilon\dot{x})^3 - 2\epsilon\dot{x}((\epsilon x + 1)^{-4} + 1) = \epsilon P\dot{x}_d \tag{27}$$

where we have taken $\gamma = 4/3$. Note that for clarity we have redefined $x_d = x(t - T)$. Next, since ϵ is a small parameter, we take the Taylor Series of Eq. (27) to obtain an expression for $\ddot{x}$ in powers of ϵ:

$$\begin{aligned}\ddot{x} = &-\frac{4xc + 4\dot{x} + P\dot{x}_d}{c} + \frac{(28x^2 - 3\dot{x}^2)c^2 + (24\,\dot{x} + 2P\dot{x}_d)xc - 8\dot{x}^2 - 2P\dot{x}_d\dot{x}}{2c^2}\epsilon \\ &- \frac{(68x^3 - 3\dot{x}^2x)c^3 + ((64\dot{x} + 2P\dot{x}_d)x^2 + 2\dot{x}^3)c^2 - (24\dot{x}^2 + 2P\dot{x}_d\dot{x})xc + 8\dot{x}^3 + 2P\dot{x}_d\dot{x}^2}{2c^3}\epsilon^2\end{aligned} \tag{28}$$

Note that in Eq. (28), the $O(\epsilon)$ and $O(\epsilon^2)$ terms are all quadratic and cubic in x, respectively. This relationship will be used later in the process of Lindstedt. We now introduce another asymptotic series that redefines time and builds a frequency-amplitude relationship into the limit cycle:

$$\tau = \Omega t \quad \Omega = \omega_{cr} + \epsilon^2 k_2 + \dots \tag{29}$$

Now is the pivotal point at which we perturb off of the critical delay. This is done to eventually retrieve an asymptotic approximation for the amplitude of the limit cycle past the Hopf bifurcation. In order to accomplish this, we set

$$T = T_{cr} + \epsilon^2 \mu \tag{30}$$

in Eq. (28), bearing in mind Eq. (29). This step is pivotal since we are not perturbing the system for small delay, but rather for small deviations from T_{cr}, as calculated from the linear analysis Eq. (23). Perturbing as such while changing the variable with respect to which we are differentiating will for instance transform terms such as

$$\begin{aligned}P\dot{x}(t - T) &= P\Omega x'(\tau - \Omega T) = P(\omega_{cr} + \epsilon^2 k_2)\underbrace{x'(\tau - \omega_{cr}T_{cr} - \epsilon^2(\omega_{cr}\mu + k_2T_{cr}) + \cdots)}_{\text{Taylor expand about}\,\tau - \omega_{cr}T_{cr}} \\ &= P\omega_{cr}x'_{d,cr} + P\epsilon^2\left(k_2x'_{d,cr} - \omega_{cr}(\omega_{cr}\mu + k_2T_{cr})x''_{d,cr}\right) + \cdots\end{aligned}$$

where $(\cdot)'$ denotes differentiation with respect to τ and $x_{d,cr} = x(\tau - \omega_{cr}T_{cr})$, due to the change of variables (29). Other terms in Eq. (28) have similar expansions resulting from the perturbation method.

As a final step in the perturbation method, the solution $x(\tau)$ is expanded in a series:

$$x(\tau) = x_0(\tau) + \epsilon x_1(\tau) + \epsilon^2 x_2(\tau) \tag{31}$$

Therefore

$$x(\tau - \omega_{cr}T_{cr}) = x_0(\tau - \omega_{cr}T_{cr}) + \epsilon x_1(\tau - \omega_{cr}T_{cr}) + \epsilon^2 x_2(\tau - \omega_{cr}T_{cr}) \tag{32}$$

Using Eqs. (31) and (32), together with the perturbations in Eqs. (30) and (29), the Taylor series expansion in Eq. (28) may be equated for the distinct orders of ϵ. This yields three equations ($O(1), O(\epsilon)$, and $O(\epsilon^2)$):

$$L(x_0) = 0 \tag{33}$$

$$L(x_1) = \frac{1}{2c^2}\left(-2(P\omega_{cr}^2x'_0 - cP\omega_{cr}x_0)x'_{0d,cr} - (3c^2 + 8)\omega_{cr}^2x_0'^2 + 24c\omega_{cr}x_0x'_0 + 28c^2x_0^2\right) \tag{34}$$

$$\begin{aligned}L(x_2) = &\frac{1}{2c^2}(2c^2\mu P\omega_{cr}^2 + 2c^2k_2PT_{cr}\omega_{cr})x''_{0d,cr} + (2c^2P\omega_{cr}x_0 - 2cP\omega_{cr}^2x'_0)x'_{1d,cr} + (2c^2P\omega_{cr}x'_{0d,cr} + 24c^2\omega_{cr}x'_0 \\ &+ 56c^3x_0)x_1 + (3c^3 + 24c)\omega_{cr}^2x_0x_0'^2 - 68c^3x_0^3 + (-2cP\omega_{cr}^2x'_{0d,cr} + (-6c^3 - 16c)\omega_{cr}^2x'_0 + 24c^2\omega_{cr}x_0)x'_1 \\ &+ (-2c^2 - 8)\omega_{cr}^3{x'_0}^3 + (-2P\omega_{cr}^3x_0'^2 + 2cP\omega_{cr}^2x_0x'_0 - 2c^2P\omega_{cr}x_0^2 - 2c^2k_2P)x'_{0d,cr} - 4c^3k_2\omega_{cr}x''_0 \\ &+ \left(-64c^2\omega_{cr}x_0^2 - 8c^2k_2x'_0\right)\end{aligned} \tag{35}$$

where

$$L(x_i) = \omega_{cr}^2 x_i'' + \frac{4\omega_{cr}}{c} x_i' + 4x_i + \frac{P\omega_{cr}}{c} x_{id,cr}$$

Eq. (33) has the solution

$$x_0(\tau) = A\sin\tau \tag{36}$$

Inserting Eq. (36) in Eq. (34) and using $x_{0d,cr} = A\sin(\tau - \omega_{cr}T_{cr})$ gives

$$\begin{aligned} L(x_1) = &-\frac{A^2P\sin(\omega_{cr}T_{cr})\omega_{cr}^2 + (-A^2c\cos(\omega_{cr}T_{cr})P - 12A^2c)\omega_{cr}}{2c^2}\sin 2\tau \\ &-\frac{(2A^2\cos(\omega_{cr}T_{cr})P + 3A^2c^2 + 8A^2)\omega_{cr}^2 + 2A^2cP\sin(\omega_{cr}T_{cr})\omega_{cr} + 28A^2c^2}{4c^2}\cos 2\tau \\ &-\frac{(2A^2\cos(\omega_{cr}T_{cr})P + 3A^2c^2 + 8A^2)\omega_{cr}^2 - 2A^2cP\sin(\omega_{cr}T_{cr})\omega_{cr} - 28A^2c^2}{4c^2} \end{aligned} \tag{37}$$

Note that Eq. (37) has no secular terms since, as mentioned above, in Eq. (28) the $O(\epsilon)$ terms are all quadratic. Next we look for a solution to Eq. (37) as:

$$x_1(\tau) = B\sin 2\tau + C\cos 2\tau + D \tag{38}$$

where the coefficients B, C and D are listed in Appendix A. Substituting Eqs. (36), (38), (43), (41) and (42) in Eq. (35) gives

$$\begin{aligned} L(x_2) = &\frac{1}{4c^3}[\sin(\omega_{cr}T_{cr})(4Ac^2\mu P\omega_{cr}^2 + 4ACcP\omega_{cr}^2 + A^3cP\omega_{cr}^2 + 4Ac^2k_2PT_{cr}\omega_{cr} + 2BAc^2P\omega_{cr}) + \cos(\omega_{cr}T_{cr}) \\ &\times(-3A^3P\omega_{cr}^3 - 4BAcP\omega_{cr}^2 + 4Ac^2DP\omega_{cr} + 2ACc^2P\omega_{cr} - A^3c^2P\omega_{cr} - 4Ac^2k_2P) + \sin(2\omega_{cr}T_{cr})(2BAc^2P\omega_{cr} \\ &- 2ACcP\omega_{cr}^2) + \cos(2\omega_{cr}T_{cr})(-2BAcP\omega_{cr}^2 - 2ACc^2P\omega_{cr}) - 12BAc^3\omega_{cr}^2 - 32BAc\omega_{cr}^2 + 48Ac^2D\omega_{cr} \\ &- 24ACc^2\omega_{cr} - 32A^3c^2\omega_{cr} - 16Ac^2k_2 + 56BAc^3 - 3A^3c^2\omega_{cr}^3 - 12A^3\omega_{cr}^3]\cos\tau + \frac{1}{8c^3}[\cos(\omega_{cr}T_{cr}) \\ &\times(-8Ac^2\mu P\omega_{cr}^2 + 8ACcP\omega_{cr}^2 + 2A^3cP\omega_{cr}^2 - 8Ac^2k_2PT_{cr}\omega_{cr} + 4BAc^2P\omega_{cr}) + \sin(\omega_{cr}T_{cr})(-2A^3P\omega_{cr}^3 \\ &+ 8BAcP\omega_{cr}^2 + 8Ac^2ccP\omega_{cr} - 4ACc^2P\omega_{cr} - 6A^3c^2P\omega_{cr} - 8Ac^2k_2P) + \cos(2\omega_{cr}T_{cr})(4ACcP\omega_{cr}^2 - 4BAc^2P\omega_{cr}) \\ &+ \sin(2\omega_{cr}T_{cr})(-4BAcP\omega_{cr}^2 - 4ACc^2P\omega_{cr}) + 24ACc^3\omega_{cr}^2 + 3A^3c^3\omega_{cr}^2 + 64ACc\omega_{cr}^2 + 24A^3c\omega_{cr}^2 + 16Ac^3k_2\omega_{cr} \\ &- 48BAc^2\omega_{cr} + 224Ac^3cc - 112ACc^3 - 204A^3c^3]\sin\tau + NRT \end{aligned} \tag{39}$$

where NRT stands for non-resonant terms. Next we remove resonant terms by setting the coefficients of $\sin\tau$ and $\cos\tau$ to zero. This yields expressions for the frequency shift k_2 and the amplitude A. These expressions are too long to list here (for example, the expression for k_2 has 154 terms when written in terms of μ, c, P, T_{cr} and ω_{cr}). For the parameters of Eqs. (15) and (24) we find:

$$k_2 = -0.639\mu, \quad A = 1.029\sqrt{\mu} \tag{40}$$

where μ is the detuning given by Eq. (30).

A comparison of the perturbation method results and the numerical results are provided in Fig. 7.

4. Conclusion

In this paper we have begun to explore the dynamics of two delay-coupled bubble oscillators, Eqs. (11) and (12), and in particular we have studied the dynamics of the in-phase mode, Eq. (13). In a classic paper, Keller and Kolodner [6] showed that the uncoupled bubble oscillator (Eq. (13) with $P = 0$) is conservative in the incompressible limit, and is damped if c is allowed to take on a finite value. Our study of the in-phase mode adds a delay feedback term to the system studied in [6]. We showed that the equilibrium can be made unstable if the delay is long enough and if the coupling coefficient P is large enough. This change in stability is accompanied by a Hopf bifurcation in which a stable periodic motion (a limit cycle) is born.

In particular, we investigated the stability of equilibrium in the in-phase mode through the use of the linear variational Eq. (14). Analysis of the characteristic Eq. (17) yielded closed form expressions for T_{cr} and ω_{cr}, Eqs. (22), (23). For values of delay T which are slightly larger than T_{cr}, we used Lindstedt's method to second order in ϵ to obtain values for the frequency and amplitude of the limit cycle.

Future work will include a study of more general dynamics of the coupled system (11), (12).

Acknowledgements

Support received from the Moroccan American Commission for Educational and Cultural Exchange through the Fulbright Program is acknowledged by author SMS. The hospitality of the Department of Theoretical and Applied Mechanics, Cornell University, is gratefully acknowledged.

CRH acknowledges the generous support of the National Science Foundation through the Graduate Research Fellowship Program. Any opinions, findings and conclusions or recommendations expressed in this publication are those of the authors and do not reflect those of the National Science Foundation.

Appendix A

The coefficients B, C and D in Eq. (38) are found to be as follows:

$$\begin{aligned} B =& [\sin(\omega_{cr}T_{cr})(8A^2cP\omega_{cr}^4 - 2A^2cP^2\omega_{cr}^2 - 24A^2cP\omega_{cr}^2) + \cos(2\omega_{cr}T_{cr})(-3A^2c^2P\omega_{cr}^3 - 8A^2P\omega_{cr}^3 - 28A^2c^2P\omega_{cr}) \\ & + \cos(\omega_{cr}T_{cr})(-8A^2c^2P\omega_{cr}^3 - 16A^2P\omega_{cr}^3 + 8A^2c^2P\omega_{cr}) + 24A^2cP\sin(2\omega_{cr}T_{cr})\omega_{cr}^2 - 2A^2cP^2\omega_{cr}^3 - 120A^2c^2\omega_{cr}^3 \\ & - 64A^2\omega_{cr}^3 - 128A^2c^2\omega_{cr}]/[64c^3\omega_{cr}^2(\omega_{cr}^2 - 2) + 4cP^2\omega_{cr}^2 + 64c\cos(2\omega_{cr}T_{cr})P\omega_{cr}^2 + 32c^2P\sin(2\omega_{cr}T_{cr})\omega_{cr}(1 - \omega_{cr}^2) \\ & + 64c(c^2 + 4\omega_{cr}^2)] \end{aligned} \tag{41}$$

$$\begin{aligned} C =& [\cos(\omega_{cr}T_{cr})(8A^2cP\omega_{cr}^4 - 24A^2cP\omega_{cr}^2) + \sin(\omega_{cr}T_{cr})(-2A^2P^2\omega_{cr}^3 + 8A^2c^2P\omega_{cr}^3 + 16A^2P\omega_{cr}^3 - 8A^2c^2P\omega_{cr}) \\ & + \sin(2\omega_{cr}T_{cr})(-3A^2c^2P\omega_{cr}^3 - 8A^2P\omega_{cr}^3 - 28A^2c^2P\omega_{cr}) - 24A^2c\cos(2\omega_{cr}T_{cr})P\omega_{cr}^2 + 100A^2c^3\omega_{cr}^2 - 224A^2c\omega_{cr}^2 \\ & - 112A^2c^3 + 12A^2c^3\omega_{cr}^4 + 32A^2c\omega_{cr}^4 - 2A^2cP^2\omega_{cr}^2]/[64c^3\omega_{cr}^2(\omega_{cr}^2 - 2) + 4cP^2\omega_{cr}^2 + 64c\cos(2\omega_{cr}T_{cr})P\omega_{cr}^2 \\ & + 32c^2P\sin(2\omega_{cr}T_{cr})\omega_{cr}(1 - \omega_{cr}^2) + 64c(c^2 + \omega_{cr}^2)] \end{aligned} \tag{42}$$

$$D = \frac{-A^2}{16c^2}(2\cos(\omega_{cr}T)P\omega_{cr}^2 - 2cP\sin(\omega_{cr}T)\omega_{cr} - 28c^2 + 3c^2\omega_{cr}^2 + 8\omega_{cr}^2) \tag{43}$$

References

[1] Dijkmans PA et al. Microbubbles and ultrasound: from diagnosis to therapy. Eur J Echocardiogr 2004;5:245–56.
[2] Doinikov AA, Manasseh R, Ooi A. Time delays in coupled multibubble systems. J Acoust Soc Am 2005;117:47–50.
[3] Ferrara K, Pollard R, Borden M. Ultrasound microbubble contrast agents: fundamentals and application to gene and drug delivery. Ann Rev Biomed Eng 2007;9:415–47.
[4] Gilmore FR. The growth or collapse of a spherical bubble in a viscous compressible liquid, Report No. 26-4. Pasadena, California: Hydrodynamics Laboratory, California Institute of Technology; 1952.
[5] Harkin A, Kaper T, Nadim A. Coupled pulsation and translation of two gas bubbles in a liquid. J Fluid Mech 2001;445:377–411.
[6] Keller JB, Kolodner II. Damping of underwater explosion bubble oscillations. J Appl Phys 1956;27:1152–61.
[7] Keller JB, Miksis M. Bubble oscillations of large amplitude. J Acoust Soc Am 1980;68:628–33.
[8] Lauterborn W, Parlitz U. Methods of chaos physics and their application to acoustics. J Acoust Soc Am 1988;84(6):1975–93.
[9] Leighton TG. From sea to surgeries, from babbling brooks to baby scans: bubble acoustics at ISVR. Proc Inst Acoust 2004;26:357–81.
[10] Manasseh R, Nikolovska A, Ooi A, Yoshida S. Anisotropy in the sound field generated by a bubble chain. J Sound Vibr 2004;278:807–82.
[11] Mettin R, Luther S, Kamphausen S, Lauterborn W. Dynamics of delay-coupled spherical bubbles. In: Lauterborn W, Kurz T, editors. Proceedings of the 15th international symposium on nonlinear acoustics Gottingen, Germany; 1–4 September 1999.
[12] Plesset MS. The dynamics of cavitation bubbles. J Appl Mech 1949;16:277–82.
[13] Plesset MS, Prosperettti A. Bubble dynamics and cavitation. Ann Rev Fluid Mech 1977;9:145–85.
[14] Rand RH. Lecture notes on nonlinear vibrations (version 52). Available online at <http://audiophile.tam.cornell.edu/randdocs>; 2007.
[15] Rand RH, Armbruster D. Perturbation methods, bifurcation theory, and computer algebra. New York: Springer-Verlag; 1987.
[16] Rand RH. Topics in nonlinear dynamics with computer algebra. Langhorne, PA: Gordon and Breach Science Publishers; 1994.
[17] Rand RH, Heckman CR. Dynamics of coupled bubble oscillators with delay. In: Proceedings of ASME 2009 IDETC/CIE 2009, San Diego, California; August 30–September 2 2009.
[18] Rayleigh, Lord. On the pressure developed in a liquid during the collapse of a spherical cavity. Phil Mag 1917;34:94–8.
[19] Reddy AJ, Szeri AJ. Coupled dynamics of translation and collapse of acoustically driven microbubbles. J Acoust Soc Am 2002;112:1346–52.
[20] Toilliez JO, Szeri AJ. Optimized translation of microbubbles driven by acoustic fields. J Acoust Soc Am 2008;123:1916–30.
[21] Wirkus S, Rand R. Dynamics of two coupled van der Pol oscillators with delay coupling. Nonlinear Dynam 2002;30:205–21.
[22] Yamakoshi Y, Ozawa Y, Ida M, Masuda N. Effects of Bjerknes forces on gas-filled microbubble trapping by ultrasonic waves. Jpn J Appl Phys 2001;40:3852–5.